

Determination of the Fermi Surface of Copper by Positron Annihilation

P. E. MIJNARENDS

Reactor Centrum Nederland, Petten, The Netherlands

(Received 12 August 1968)

The momentum distribution of annihilation radiation in copper has been determined by unfolding eight accurately measured angular correlations following a new method. The core contribution is found to be anisotropic with a minimum in the [100] directions. The Fermi radii are determined from the half-width of the conduction-electron contribution. Except in the [110] directions, where its radius is at least 5% too large, the shape of the Fermi surface agrees with that obtained from measurements of the de Haas-van Alphen effect. A tentative explanation is offered in terms of a local perturbation of the electron band structure by the positron-electron interaction.

1. INTRODUCTION

DURING the past few years studies of positron annihilation in oriented single crystals of metals have aimed at the determination of the shape of the Fermi surface.¹⁻⁴ Usually one observes the angular correlation of the annihilation radiation as a function of sample orientation with a long-slit setup. The cutoff angle of the central parabolic part of the angular correlation is then considered to be a measure for the Fermi momentum in that specific direction. In simple metals like the alkali metals, where the contribution of the annihilations with the core electrons is small and can easily be separated from the parabolic part, this method gives reliable results.⁴ In metals with a more complicated electronic structure like the transition metals, this method is often more difficult to apply.

Recently a new method⁵ has been suggested to unfold the angular correlations, yielding the momentum distribution of the pairs of annihilation quanta. This anisotropic distribution shows a large discontinuity at the Fermi momentum, smeared out only by the instrumental resolution and the motion of the positron.^{6,7} From the variation of the half-width of this momentum distribution with orientation, it should, in principle, be possible to obtain a precise value of the radius of the Fermi surface in all directions. The applicability of this procedure was illustrated by a model computation.

In order to further investigate the capabilities of the method given in I it was decided to apply it to a real metal having a sufficiently anisotropic Fermi surface. The choice of the metal was further dictated by the requirement that a large amount of information concerning its Fermi surface, experimental as well as

theoretical, should be available from other sources in order to allow a comparison of the results obtained. Copper, being one of the few metals satisfying both requirements, was chosen for this purpose. It has been studied extensively with the aid of many different techniques, including positron annihilation,⁸⁻¹⁰ and has the added advantage that sufficiently large single crystals can be grown of it, such that a large number of differently oriented samples can be cut from one ingot.

The present paper describes the results of a careful measurement of the angular correlations for eight different sample orientations. The correlations are transformed into the momentum distribution of the annihilation quanta, from which the shape of the Fermi surface is derived. For the purpose of easy reference Sec. 2 gives the formulas needed for this transformation; for a full discussion of the underlying theory the reader is referred to I. Section 3 gives a short description of the experimental procedure, while in Sec. 4 some of the necessary corrections are discussed. In Sec. 5 the results are presented and discussed.

2. THEORY

The two-quantum angular correlation $N(p_z)$, measured with a horizontal long-slit setup, is proportional to the probability that the pair of annihilation quanta carries off a momentum with a component along the vertical z axis of the instrument between p_z and $p_z + dp_z$. This probability is related to the momentum distribution $\rho(\mathbf{p})$ of the photon pair by

$$N(p_z) \propto \int_{-\infty}^{\infty} \int_{-\infty}^{\infty} \rho(\mathbf{p}) dp_x dp_y = \int_0^{2\pi} \int_{|p_z|}^{\infty} \rho(\mathbf{p}) p dp d\phi, \quad (1)$$

where ϕ represents the azimuthal angle around the z axis of the instrument.

As $\rho(\mathbf{p})$ possesses the same point symmetry as the crystal lattice, it can for copper be expanded in Kubic

¹ A. T. Stewart, J. B. Shand, J. J. Donaghy, and J. H. Kusmiss, *Phys. Rev.* **128**, 118 (1962).

² R. W. Williams, T. L. Loucks, and A. R. Mackintosh, *Phys. Rev. Letters* **16**, 168 (1966).

³ K. Fujiwara and O. Sueoka, *J. Phys. Soc. Japan* **21**, 1947 (1966); **23**, 1242 (1967).

⁴ J. J. Donaghy and A. T. Stewart, *Phys. Rev.* **164**, 391 (1967); **164**, 396 (1967).

⁵ P. E. Mijnenrens, *Phys. Rev.* **160**, 512 (1967), hereafter referred to as I.

⁶ A. T. Stewart and J. B. Shand, *Phys. Rev. Letters* **16**, 261 (1966).

⁷ S. M. Kim, A. T. Stewart, and J. P. Carbotte, *Phys. Rev. Letters* **18**, 385 (1967).

⁸ S. Berko and J. S. Plaskett, *Phys. Rev.* **112**, 1877 (1958).

⁹ O. Sueoka, *J. Phys. Soc. Japan* **23**, 1246 (1967).

¹⁰ D. L. Williams, E. H. Becker, P. Petievich, and G. Jones, *Phys. Rev. Letters* **20**, 448 (1968).

harmonics $K_{l\nu}(\Omega)$ of α type¹¹:

$$\rho(\mathbf{p}) = \sum_{l\nu} \rho_{l\nu}(\mathbf{p}) K_{l\nu}(\Omega). \quad (2)$$

ν is an index distinguishing the various harmonics of the same order and symmetry type, and will be dropped in the following. Substitution into Eq. (1) and integration with respect to ϕ yields

$$N_{\beta,\alpha}(p_z) \propto \sum_l K_l(\beta,\alpha) g_l(p_z), \quad (3)$$

where β and α , respectively, represent the polar and azimuthal angle of the z axis of the instrument with respect to the crystalline coordinate system, and

$$g_l(p_z) = \int_{|p_z|}^{\infty} \rho_l(p) P_l(p_z/p) p dp. \quad (4)$$

If the angular correlation is measured for n different sample orientations β, α , Eq. (3) represents a system of n linear equations with the $g_l(p_z)$ as unknowns. Truncation at a certain value of l and inversion of this system yields the $g_l(p_z)$ expressed as linear combinations of the n observed angular correlations:

$$g_l(p_z) = \sum_{\beta,\alpha} c_l(\beta,\alpha) N_{\beta,\alpha}(p_z). \quad (5)$$

Solution of the integral Eq. (4) then allows one to express the $\rho_l(p)$ in terms of $g_l(p)$, according to

$$\rho_l(p) = -\frac{1}{p} \left[\frac{dg_l(p)}{dp} - \frac{l(l+1)}{2p} g_l(p) + \frac{1}{p^2} \int_0^p g_l(z) P_l''(z/p) dz \right], \quad (6)$$

after which Eq. (2) permits the construction of the momentum density function $\rho(\mathbf{p})$.

3. EXPERIMENT

The apparatus used for the experiment is similar to other setups described in the literature,¹² and has been automated as far as possible. The detectors, placed at a distance of 3 m from the sample, consist of 12-in.-long NaI(Tl) crystals, coupled on both sides to photomultipliers. The positrons, generated by 100 mCi of Na²², are magnetically focused onto the sample, which is placed in a vacuum chamber in order to prevent oxidation of the surface.

The samples consist of parallelepipeds of about 25×7×6 mm³, cut by spark erosion from a large single crystal of copper of 99.99% purity. After having been cut and etched, the crystals were annealed by heating

¹¹ F. C. Von der Lage and H. A. Bethe, Phys. Rev. **71**, 612 (1947); F. M. Mueller and M. G. Priestley, *ibid.* **148**, 638 (1966).

¹² D. R. Gustafson, A. R. Mackintosh, and D. J. Zaffarano, Phys. Rev. **130**, 1455 (1963).

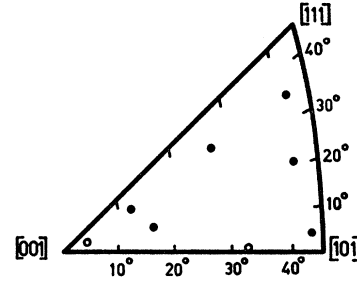


FIG. 1. Stereographic plot of the sample orientations. Full circles: high and low resolution; open circles: high resolution only.

to 400°C during 24 h, followed by slow cooling to room temperature and a second etching. The eight sample orientations, determined by means of Laue back reflection, cover the spherical triangle between the [001], [101], and [111] directions more or less evenly, as shown in Fig. 1, and are believed to be accurate within a few tenths of a degree.

For each sample, data were taken at 0.2 mrad intervals, and the range of interest was scanned many times. The background amounted to about 1% of the peak coincidence rate. In order to make the absorption of the annihilation radiation independent of the position of the movable detector over most of the range of interest, the samples were not mounted exactly horizontal, but under an angle of about 3° with respect to the horizontal line connecting the detectors at $\theta = p_z/mc = 0$. This tilt is included in the orientations indicated in Fig. 1. The angular correlations were corrected for the slight residual dependence on angle.

4. CORRECTIONS

Several corrections were applied to the data before Eqs. (2)–(6) could be used to yield the momentum distribution of the annihilation radiation. After subtraction of the background and correction for the angle-dependent absorption in the sample, the center of the peak was determined in three different ways: (a) By determination of the center of gravity; (b) by determination of the zero-crossing of its derivative; and (c) by drawing a number of horizontal chords and taking the average of the points of intersection of these chords with the peak. These methods gave results differing by as much as 0.1 mrad for some peaks.

If the peaks were folded about their center of gravity, in each instance a slight asymmetry became apparent, caused by the penetration and exponential attenuation of the positrons in the sample. Annihilations taking place in a layer between z and $z+dz$ below the sample surface give rise to an annihilation peak, which is shifted over an angle of $2z/L$ mrad and attenuated by a factor $e^{-\alpha z}$ with respect to the contribution from the sample surface. Here α represents the absorption coefficient of the positron beam in the sample, while L denotes the sample-detector distance. Since the ob-

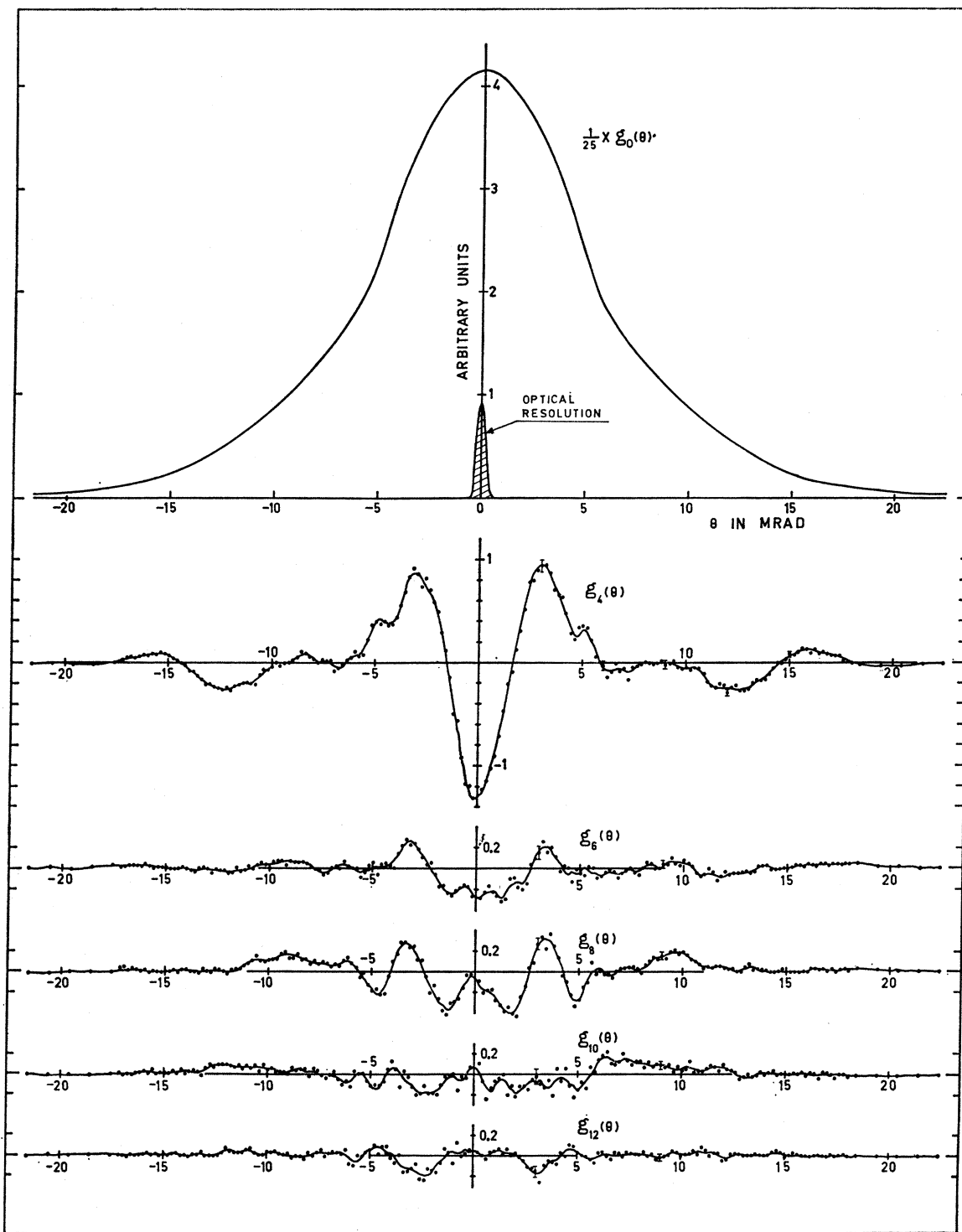


FIG. 2. The first six g_l functions, computed by retaining the first six terms in Eq. (3) and neglecting the higher ones. The points have been obtained by parabolic interpolation of the raw data without smoothing, and therefore are representative for the raw data. The drawn curves represent the result of local smoothing by fitting parabolas to seven adjacent points. The individual points of $g_0(\theta)$ have been omitted since their accuracy is far within the line thickness. Note the scale factor in front of $g_0(\theta)$.

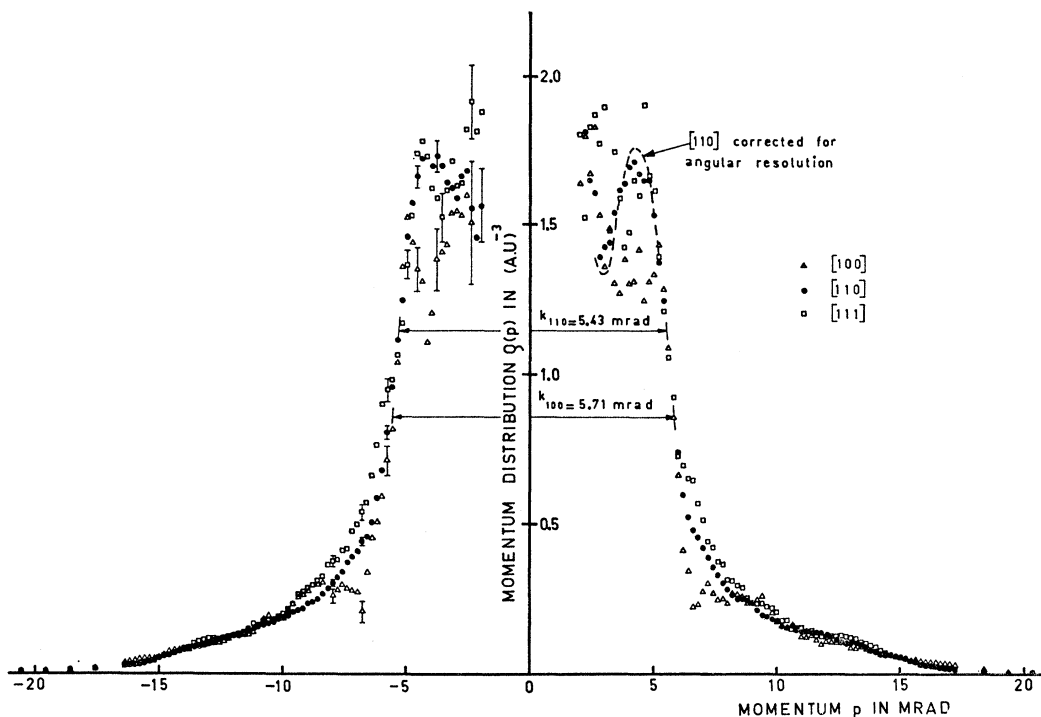


Fig. 3. Momentum distribution $\rho(p)$ along the [100], [110], and [111] axes, computed from the g_l functions shown in Fig. 2.

served angular correlation is a superposition of all of these partial correlations, a slight asymmetry will be the result. Owing to the severe attenuation of a positron beam in solid matter this effect will be small if the sample surface is ideally flat and horizontal. The heavy etching of the crystals, however, produced a slightly convex surface, which, when tilted over a small angle, has the same effect as a significant increase in positron penetration depth. In the Appendix it is shown that in the hypothetical case of a Gaussian peak shape and an exponential positron attenuation the resulting asymmetry may be corrected to first order by multiplication of the correlation by a factor $1 - a\theta$, with $a = 4\lambda^2/\alpha L$, where λ denotes half the full width at half maximum (FWHM) of the angular correlation. This justifies the empirical procedure adopted in this experiment of symmetrizing the correlations by multiplying them by a factor $1 - a\theta$, where the parameter a in each case is chosen such as to give the best possible overlap (in an east-squares sense) between the left- and the right-hand part of the correlation. The result of this procedure is a great improvement in the symmetry of the correlations, and consequently a much closer agreement (generally better than 0.02 mrad) between the peak centers determined in the three ways described above.

Subsequently, starting from the center of each correlation, to which was assigned the abscissa $\theta = 0$, points at intervals of 0.2 mrad were computed by interpolation from the observed angular correlations. In this interpolation process some slight local smoothing

was applied at the same time by fitting a parabola to a number of points, and repeating this process for each point of the correlation. The correlations were normalized by computing the area under the resulting curves and correcting for the fact that the coincidence rate in the wings had not quite come down to the background yet.

After the eight angular correlations had been corrected and smoothed in this way, Eq. (3) was truncated after the desired number of terms, and the g_l functions computed according to Eq. (5). Standard least-squares techniques¹³ were used to evaluate the coefficients $c_l(\beta, \alpha)$. Figure 2 shows a set of g_l 's up to $l = 12$, obtained by retaining the first six terms in Eq. (3) and neglecting the higher ones. These functions were inserted into Eq. (6) and the corresponding ρ_l 's computed from them. The differentiation in the first term was accomplished numerically by use of a 7-point formula. The total momentum distribution $\rho(p)$ was finally constructed from Eq. (2) and is shown in Fig. 3. The error bars represent the errors due to counting statistics and were computed from the law of error propagation, taking account of the many ways in which the final data were mutually correlated.

The data were analyzed in several ways, by varying the amount of smoothing applied to the original angular correlations, the number of terms retained in Eq. (3), and the number of neighboring datum points used in

¹³ C. Lanczos, *Applied Analysis* (Sir Isaac Pitman & Sons, Ltd., London, 1964), Chap. II.

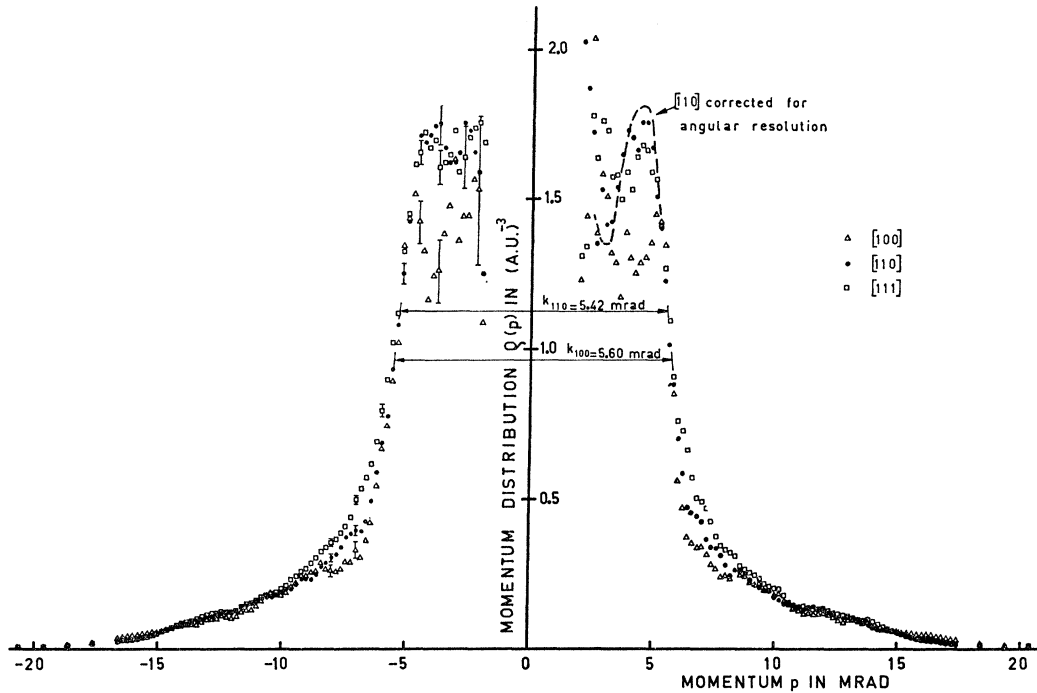


FIG. 4. As Fig. 3, but computed by retaining the first four terms in Eq. (3) ($l \leq 8$), and applying less smoothing.

the differentiation in Eq. (6). This gave some insight in the amount of information which can be extracted from the present data. For instance, breaking off the series Eq. (3) after $l=8$, and use of less smoothing (by fitting a parabola to 5 points instead of 7) did not give essentially different results, as may be seen from comparison of Figs. 3 and 4.

Finally, a correction was made for the finite angular resolution (0.56 mrad) of the apparatus.¹⁴ By repeating the measurement of six of the angular correlations with an optical resolution of 1.5 mrad, the influence of the angular resolution was also investigated experimentally.

The numerous computations needed for the data analysis were performed on an Electrologica X8 digital computer, to which end a series of ALGOL programs was written.

5. RESULTS AND DISCUSSION

The g_l functions plotted in Fig. 2 show a considerable amount of structure. The symmetry displayed by them, although by no means perfect, demonstrates the effectiveness of the correction procedure described in Sec. 4, since it should be realized that each function with $l \neq 0$ has an amplitude of about 1% of that of the eight angular correlations, which were combined to obtain them. When uncorrected correlations were used $g_6(\theta)$ turned out to be antisymmetric rather than symmetric.

The most striking feature in the total momentum distribution $\rho(\mathbf{p})$ as plotted in Figs. 3 and 4, is the

marked anisotropy of the core electron contribution, expected to originate mainly from the 3d electrons. In the single-particle picture $\rho(\mathbf{p})$ may be written

$$\rho(\mathbf{p}) = \text{const} \times \sum_{\mathbf{k}} f(\mathbf{k}) |\chi(\mathbf{k}, \mathbf{p})|^2, \quad (7)$$

with

$$\chi(\mathbf{k}, \mathbf{p}) = \int_{\text{crystal}} e^{-i\mathbf{p} \cdot \mathbf{r}} \psi_{\mathbf{k}}(\mathbf{r}) \phi_+(\mathbf{r}) d\mathbf{r}, \quad (8)$$

$\phi_+(\mathbf{r})$ representing the positron wave function, while $\psi_{\mathbf{k}}(\mathbf{r})$ is a Bloch function for an electron with crystal momentum \mathbf{k} . The occupation function $f(\mathbf{k})$ takes the values 1 or 0 according to whether the state \mathbf{k} is occupied or empty. If it is assumed that for the conduction states $|\chi(\mathbf{k}, \mathbf{p})|^2$ is not strongly anisotropic, then the considerable decrease in $\rho(\mathbf{p})$ in the [100] directions, also at momenta $p < k_F$, must reflect a corresponding anisotropy of the core contribution. In the [111] directions on the other hand, $\rho(\mathbf{p})$ shows a maximum. These are the directions in which the distance to the Brillouin zone boundary is a minimum, so some contribution from Umklapp processes may be present, but just how much is difficult to assess unambiguously from the present data. It can then be concluded that the core contribution is probably little different in the [110] and [111] directions, but is lower by some 30 to 50% along [100].

Secondly the contour plot in Fig. 5 clearly shows the presence of necks along [111], piercing the zone face. The momentum density inside these necks is considerably smaller than in the belly, in accordance with

¹⁴ C. Eckart, Phys. Rev. **51**, 735 (1937).

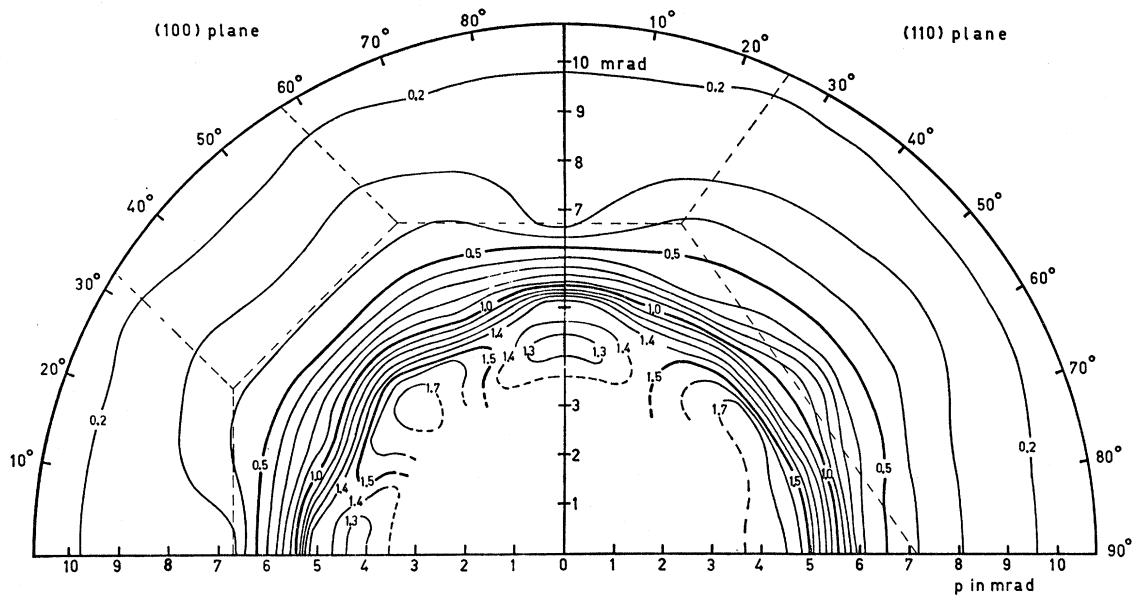


FIG. 5. Central part of the momentum distribution $\rho(\mathbf{p})$ [in (a.u.)⁻³] in the (100) and (110) planes.

the nearly free-electron calculation of Berko and Plaskett.⁸

The role played by enhancement is not quite clear. On the basis of Kahana's free-electron theory¹⁵ one computes $\epsilon(\mathbf{k}_F)/\epsilon(0)=1.3$ for copper. In how far this theory would hold in the case of real metals is not known. Figures 3 and 4 indeed display a certain peaking of the momentum density at \mathbf{k}_F , which is assumed to reflect the effect of enhancement. The enhancement factor displays anisotropy because the observed peaking is not equally strong in every direction. By means of model computations of the kind described in I, it was ascertained that the observed peaks are not a trivial series termination effect.

It is well known that for reasons of geometry the long-slit apparatus does not yield accurate information about the behavior of $\rho(\mathbf{p})$ at $\mathbf{p}\approx 0$. Comparison of the normalized angular correlations measured with resolutions of 0.56 and 1.5 mrad, however, showed that all low-resolution curves were 2% higher at $\theta=0$ than the corresponding ones taken with a resolution of 0.56 mrad. This indicates that $\rho(\mathbf{p})$ drops fairly sharply at small momenta, as is to be expected since at $\mathbf{p}=0$ only s states can contribute.

Next the computed momentum distribution was used to determine the Fermi radius in all directions. This was done by estimating the bottom and the top of the slope at \mathbf{k}_F as well as possible (taking the instrumental resolution into account), and measuring the diameter of the central part of the distribution halfway between these points. Admittedly, a considerable amount of arbitrariness is involved in this determination, but nevertheless

¹⁵ S. Kahana, Phys. Rev. **117**, 123 (1960); **129**, 1622 (1963).

it is believed that the uncertainty in estimating the point at which to measure the diameter will not be more than ± 0.1 (a.u.)⁻³, corresponding to an error of ± 0.11 mrad or about 2% in \mathbf{k}_F (the statistical error varies with direction from 0.3 to 0.6% and can therefore be neglected). The radii obtained in this way are shown in Fig. 6 (full circles). Taking a value of $3.615 \text{ \AA} = 6.831$ a.u. for the lattice constant, the volume of this Fermi surface, after correction for the necks, corresponds to about 1.06 electrons per atom, i.e., the radii are on the

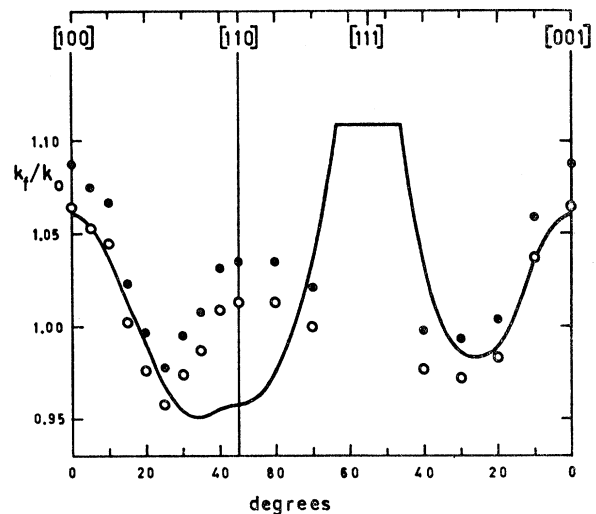


FIG. 6. Ratio of Fermi radius k_F , obtained from the 6-term analysis of $\rho(\mathbf{p})$, to the free-electron Fermi radius k_0 (full circles) in the (001) and (110) planes. The drawn curve represents the results of a de Haas-van Alphen experiment (Refs. 16 and 17). The open circles are obtained by reducing the volume of the Fermi surface to 1 electron/atom.

average 2% larger than expected. The drawn lines represent the results of measurements of the de Haas-van Alphen effect in copper, performed by Joseph *et al.*,¹⁶ and analyzed in terms of Kubic harmonics by Zornberg and Mueller.¹⁷ If the radii obtained in the present work are reduced by 2% the open circles result, which in the neighborhood of the [100] directions agree very well with the de Haas-van Alphen data. The radii near [110] are still about 5% too large, however. Altogether the observed surface seems to be more spherical.

The question arises how significant these deviations are. The difference in k_{110} is certainly far outside the 2% uncertainty due to a possible systematic error in the estimate of the height at which to determine the Fermi radius. In fact, examination of Figs. 3 and 4 shows that one would have to measure the diameter at an unrealistically high point to reproduce the de Haas-van Alphen value. On the other hand it might be surmised that the disagreement could be caused by the neglect of all harmonics with $l > 12$ (in the analysis of Zornberg and Mueller harmonics up to $l = 18$ were used). Although this possibility cannot be ruled out entirely, it becomes very unlikely if one compares the results of the six-term analysis employed to obtain the present data with the results of the analysis in which only 4 terms ($l \leq 8$) are used (Table I). The differences, if any, are remarkably small. One must conclude therefore that k_{110} deviates significantly from its expected value.

The significance of the disagreement in Fermi surface volume is less certain. The presence of a sharp peak in $\rho(\mathbf{p})$ at the Fermi surface, caused by enhancement, makes the value of k_F sensitive to the accuracy with which the correction for finite angular resolution can be carried out. An incomplete correction, for instance, by neglecting positron motion, would tend to produce a Fermi radius which is slightly too large. Since this would hold for all directions, the effect on the volume is quite

TABLE I. Fermi radii k_F (in mrad) and Fermi surface volume (in electrons per atom) determined from the momentum distribution $\rho(\mathbf{p})$, obtained by retaining, respectively, 4 or 6 terms in Eq. (2). The angle θ is measured from the [001] axis.

Angle ϕ in (001) plane	k_F		Angle θ in (110) plane	k_F	
	4 terms	6 terms		4 terms	6 terms
0°	5.60	5.71	0°	5.60	5.71
5°	5.61	5.64	10°	5.56	5.56
10°	5.56	5.60	20°	5.25	5.27
15°	5.43	5.37	30°	5.17	5.21
20°	5.33	5.23	40°	5.24	5.24
25°	5.22	5.13	50°	neck	neck
30°	5.26	5.22	60°	neck	neck
35°	5.32	5.29	70°	5.36	5.36
40°	5.40	5.41	80°	5.38	5.43
45°	5.42	5.43	90°	5.42	5.43
	Volume		4 terms	1.061	
	(electrons/atom)		6 terms	1.065	

¹⁶ A. S. Joseph, A. C. Thorsen, E. Gertner, and L. E. Valby, *Phys. Rev.* **148**, 569 (1966).

¹⁷ E. I. Zornberg and F. M. Mueller, *Phys. Rev.* **151**, 557 (1966).

serious. It demonstrates the necessity of using a high angular resolution in the present type of experiment, eventually combined with cooling of the sample to reduce positron motion. In the second place the possibility of an important error committed in separating the core contribution from the contribution of the conduction electrons, though unlikely, cannot altogether be excluded. This separation has proved to be a difficult point in many recent angular correlation studies, especially if it is attempted to draw conclusions from the angular correlation itself. The situation is somewhat alleviated if one first effects the transformation to $\rho(\mathbf{p})$, since this essentially corresponds to a differentiation of the experimental data, which makes the small details more clearly visible. Yet one would feel more comfortable if there existed an augmented-plane-wave (APW) calculation of $\rho(\mathbf{p})$ to act as a guide in the separation process. These arguments suggest that no definite conclusions can be derived from the difference in Fermi surface volume.

It is of interest to compare the present results with those obtained by means of the rotating specimen method, which were recently reported by Williams *et al.*¹⁰ In this technique the observed coincidence rate for a chosen sample orientation is proportional to $\int \rho(\mathbf{p}) d\mathbf{p}$, integrated along a diameter of the momentum distribution. Ideally this quantity equals the area under the corresponding curve in Fig. 3. They compared their data with a model of the Fermi surface, and concluded that the core electrons contribute equally along [100] and [111], but give a markedly larger contribution along [110]. The present data indicate that it is probably more correct to ascribe the bumps, which they observed in the [111] directions, partly to the necks, and partly to Umklapp processes caused by the higher momentum components in the positron and electron wave functions, while the disagreement between calculation and experiment in the [110] directions is caused to a great extent by the apparent distortion of the Fermi surface in those directions.

It remains to explain why the shape of the Fermi surface is somewhat different from that observed by other methods. From the foregoing arguments it follows that the independent-particle model is inadequate for this purpose. It is known from lifetime measurements, however, that the positron profoundly perturbs the surrounding electron gas. An electron cloud is formed around it, screening the long range part of the positron Coulomb potential, and the enhanced electron density results in a greatly reduced positron lifetime. A proper treatment should therefore include these many-body effects. Theoretical studies of the combined effects of electron-electron and positron-electron correlation on the angular correlations are scarce, however. The most extensive study is due to Majumdar,¹⁸ who, on the

¹⁸ C. K. Majumdar, *Phys. Rev.* **140**, A227 (1965); **140**, A237 (1965).

basis of perturbation theory, showed that a break in the angular correlation curve will occur at a momentum corresponding to the Fermi energy, i.e., at the Fermi surface.

The following speculation could now be made. The positron, together with its electron cloud, represents a local distortion of the potential $V(\mathbf{r})$ in the metal. Since the detailed form of the electron band structure $E(\mathbf{k})$ depends on this potential it does not seem unreasonable to assume that at the center of the electron cloud $E(\mathbf{k})$ is somewhat different from the value in the rest of the metal. In an anisotropic crystal the same will then be true of the shape of the Fermi surface. Consequently the positron, always being at the point of maximum deformation, would by its annihilation provide information about this local Fermi surface, and not directly about the Fermi surface existing in the bulk of the metal.

Earlier positron results are not in conflict with this conclusion as one must expect that the local Fermi surface will be most distorted in highly anisotropic metals, the angular correlations of which have hitherto been little amenable to detailed and unambiguous interpretation. Recent successes⁴ in the determination of Fermi surface shapes have been achieved in fairly isotropic metals as lithium. For further confirmation and a better understanding of the effect it would be desirable that the present experiment be repeated on highly anisotropic metals as beryllium or the rare earths.

After this work was concluded we learned that Williams and Mackintosh¹⁹ have observed a certain blurring of the structure in their calculated angular correlations for Y and a number of rare earths. They give a tentative explanation in terms of a decrease in the anisotropy of the conduction-electron gas in the vicinity of the positron due to the Coulomb correlation, thus strengthening the conclusion of the present paper.

ACKNOWLEDGMENTS

The author wishes to express his great appreciation to Dr. B. O. Loopstra for his kind interest and stimulating criticism during every stage of the work. He would also like to thank Professor M. Dresden for an interesting conversation. The technical assistance of G. J. Langedijk is much appreciated. The author is also much indebted to the staff of the electronics department, especially C. F. A. Frumau and J. Muller, and to S. Slagter and R. J. Scheper for the design and assembly of the equipment.

APPENDIX

Annihilation quanta created by positrons annihilating at the very surface of the sample (i.e., at $z=0$), will give

¹⁹ R. W. Williams and A. R. Mackintosh, Phys. Rev. **168**, 679 (1968).

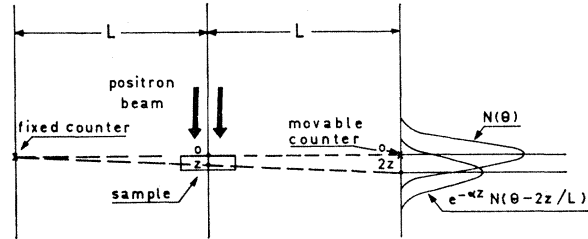


FIG. 7. Peak asymmetry due to positron penetration in the sample (not to scale).

rise, in the absence of any γ -ray absorption in the sample, to a symmetric angular correlation $N(\theta)$ with its center at $\theta=0$ (Fig. 7). A fraction $e^{-\alpha z} dz$ of the positron beam will annihilate at a depth between z and $z+dz$, and give a similar contribution, but shifted over an angle $\theta=2z/L$, and less intense by a factor $e^{-\alpha z}$. The total angular correlation observed by the apparatus will therefore have the form

$$N_{\text{obs}}(\theta) = \alpha \int_0^{\infty} N(\theta - 2z/L) e^{-\alpha z} dz, \quad (\text{A1})$$

which is no longer symmetric.

Some insight in the form of the asymmetry may be obtained if it is assumed that the shape of the undistorted angular correlation can be approximated by a Gaussian:

$$N_{\text{true}}(\theta) = N_0 \exp(-\lambda^2 \theta^2).$$

Then²⁰

$$\begin{aligned} N_{\text{obs}}(\theta) &= \alpha N_0 \int_0^{\infty} \exp[-\lambda^2 (\theta - 2z/L)^2] e^{-\alpha z} dz \\ &= \pi^{1/2} \xi N_0 \exp(\xi^2 - 2\xi\lambda\theta) [1 - \Phi(\xi - \lambda\theta)], \end{aligned} \quad (\text{A2})$$

where $\xi = \alpha L / 4\lambda$ and $\Phi(y) = 2\pi^{-1/2} \int_0^y \exp(-t^2) dt$ represents the error function. In a typical experiment the quantity $y = \xi - \lambda\theta$ is of the order 50, so to a fair approximation $1 - \Phi(y)$ may be replaced by the first term of its asymptotic expansion²¹

$$1 - \Phi(y) \sim \pi^{-1/2} y^{-1} \exp(-y^2).$$

Substitution into Eq. (A2) yields

$$N_{\text{obs}}(\theta) \sim (1 - \lambda\theta/\xi)^{-1} N_{\text{true}}(\theta). \quad (\text{A3})$$

It therefore follows that the asymmetry may be corrected to first order by multiplication of the observed angular correlation by a factor $1 - \lambda\theta/\xi = 1 - (4\lambda^2/\alpha L)\theta$.

²⁰ I. S. Gradshteyn and I. M. Ryzhik, *Tables of Integrals, Series, and Products* (Academic Press Inc., New York, 1965), p. 307.

²¹ Reference 20, p. 931.